Direct Absolute pK(a) Predictions and Proton Transfer Mechanisms of Small Molecules in Aqueous Solution by QM/MM-MD

ARTICLE *in* THE JOURNAL OF PHYSICAL CHEMISTRY B · APRIL 2013

Impact Factor: 3.3 · DOI: 10.1021/jp400180x · Source: PubMed

3 AUTHORS:

Nizam Uddin
Kyungpook National University
6 PUBLICATIONS **38** CITATIONS
SEE PROFILE

Tae Hoon Choi
Chungnam National University
23 PUBLICATIONS **122** CITATIONS
SEE PROFILE

Cheol Ho Choi
Kyungpook National University
111 PUBLICATIONS **2,123** CITATIONS
SEE PROFILE

THE JOURNAL OF PHYSICAL CHEMISTRY B

Article

pubs.acs.org/JPCB

Direct Absolute pK_a Predictions and Proton Transfer Mechanisms of Small Molecules in Aqueous Solution by QM/MM-MD

Nizam Uddin,[†] Tae Hoon Choi,*[,‡] and Cheol Ho Choi*[,†]

[†]Department of Chemistry and Green-Nano Materials Research Center, College of Natural Sciences, Kyungpook National University, Taegu 702-701, South Korea

[‡]Department of Chemical Engineering Education, Chungnam National University, Daejeon 305-764, South Korea

Supporting Information

ABSTRACT: The pK_a values of HF, HCOOH, CH_3COOH, CH_3CH_2COOH, H_2CO_3, HOCl, NH_4^+, $CH_3NH_3^+$, H_2O_2, and CH_3CH_2OH in aqueous solution were predicted by QM/MM-MD in combination with umbrella samplings adopting the flexible asymmetric coordinate (FAC). This unique combination yielded remarkably accurate values with the maximum and root-mean-square errors of 0.45 and 0.22 in pK_a units, respectively, without any numerical or experimental adjustments. The stability of the initially formed Coulomb pair rather than the proton transfer stage turned out to be the rate-determining step, implying that the stabilizations of the created ions require a large free energy increase. A remarkable correlation between DWR (degree of water rearrangements) and pK_a was observed. As such, the large pK_a of ethanol can be, in part, attributed to the large water rearrangement, strongly suggesting that proper samplings of water dynamics at dissociated regions are critical for accurate predictions of pK_a. Current results exhibit a promising protocol for direct and accurate predictions of pK_a. The significant variations in the gas phase deprotonation energies with level of theory appear to be mostly canceled by the similar changes in the averaged solute−solvent interactions, yielding accurate results.

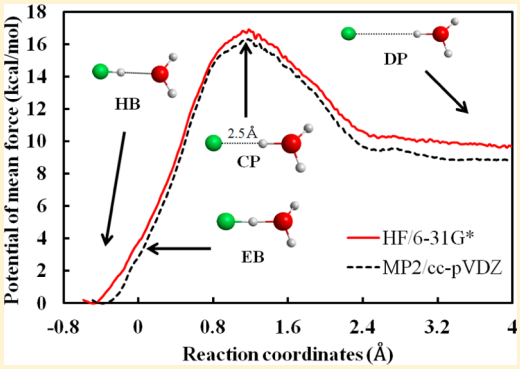

1. INTRODUCTION

Accurate calculation of pK_a values for ubiquitous acid/base reactions has been a central goal of theoretical chemistry. The prediction accuracy within 0.5 pK_a units of experiment[1,2] is the desirable level of accuracy for many problems. The majority of pK_a calculations of solvated molecules have been performed on the model systems of quantum mechanical solute with the electric continuum models.[1,3−24] As the recent extensive review shows,[25] the deprotonation free energy is expressed as the sum of the deprotonation free energy of the molecule in the gas phase and the solvation free energy difference of products and the reactant using thermodynamic cycles. Although this scheme can take advantage of high-level ab initio methods for the deprotonation step, local solvation dynamics such as the direct hydrogen bonding effects are not explicitly accounted for. Ho and Coote[25] summarized that the reference-independent hybrid approaches can potentially give reasonably accurate values (∼2 units accuracy in pK_a) depending on the solvent model and the number of explicit water molecules added. Hybrid approaches[17,18,22,23,25−27] have been attempted to capture the missing first and sometimes second solvation shell directed effects in the presence of a continuum model. As a systematic approach, Abramson and Baldrigde[28] introduced the defined-sector explicit solvent in continuum cluster (DSES-CC) model approach, relying only on solution phase computation (i.e., eliminating use of a thermodynamic cycle) and the use of the sector model for placement of explicit solvent molecules.

An alternative to QM-continuum computations is ab initio molecular dynamics (AIMD) calculation of pK_a.[29−32] In contrast to QM-continuum methods, in the AIMD approach, both the solute and the solvent are treated quantum mechanically, and the deprotonation free energy can be obtained from the statistical mechanics formalism of condensed phase simulation. The advantage of AIMD is that the local solute−solvent dynamics are properly accounted for at the same QM level of theory. However due to the significantly increased computational overhead, the number of solvents and simulation time are rather limited.

Classical MD studies suggested[33] that simulations for 100−200 ps are necessary to obtain converged hydration dynamics. Although AIMD simulations such as CPMD[34] or FMO-MD[35] can provide the most direct tool for studying proton transfer, simulations over such time scales for systems with sufficient size are still difficult. To overcome this challenge, the quantum mechanical/molecular mechanical (QM/MM) method is often utilized.[36] This approach can be especially useful in the case of chemical reactions in solutions, where a clear boundary

Received: January 6, 2013
Revised: April 6, 2013
Published: April 21, 2013

   dx.doi.org/10.1021/jp400180x | J. Phys. Chem. B 2013, 117, 6269−6275

between solute and solvents exists. As one of the improved versions of QM/MM, the applicability of the hybrid QM/EFP to a long-time MD simulation of chemical reaction in aqueous solution has recently been examined.[37] This also showed that sampling on the order of ~100 ps is needed to properly describe the local hydrogen bonding dynamics. The same approach has also been successfully utilized for NaCl association/dissociation dynamics,[38] hydrophobic association of methanol dimer,[39] and anharmonic vibrational properties[40] in aqueous solutions. In the study of anharmonic vibrational properties, a TIP5P[41] water model was also successfully adopted. One of the important terms of the hybrid method is the coupling interaction between QM and MM. The effective Gaussian repulsion potentials similar to those of the EFP1-HF model were used for the coupling interaction between QM and TIP5P. The detailed descriptions of our approach can be found in the previous papers. In short, the unique combination of the hybrid QM/EFP and QM/TIP5P and the traditional sampling techniques can be a both practical and highly accurate route for solvation dynamics. These approaches comprise QM-QM, QM-MM, and MM-MM interaction terms, which are ingredients for the correct dynamic descriptions of solute in solvents. In this work, the same QM/TIP5P-MD approach shall be utilized for the direct pK_a predictions of HF, HCOOH, CH_3COOH, CH_3CH_2COOH, H_2CO_3, HOCl, NH_4^+, $CH_3NH_3^+$, H_2O_2, and CH_3CH_2OH in aqueous solution. These 10 molecules were carefully chosen to cover the wide pK_a range of 3−16.

The essential quantity required for the pK_a prediction of a given molecule in aqueous solution is the Helmholtz free energy difference for hydrogen abstraction by water,

$$HA + H_2O \rightarrow A^- + H_3O^+ \quad (1)$$

It can be extracted from constrained molecular dynamics such as umbrella sampling technique provided that the control parameter is a reasonable approximation to the true reaction coordinate. However, in high dimensional systems, a simple distance constraint often yields a rather poor approximation to the true reaction coordinate, and can lead to erroneous results.[42] An additional problem is encountered in multifunctional molecules such as acetic acid, where the dissociating proton can be readsorbed to the other oxygen of the same molecule.

In order to overcome these complications, a flexible asymmetric coordinate (FAC) is introduced in this work. The asymmetric coordinate ($R_{A-H} - R_{O^*-H}$) has been successfully applied to the intramolecular proton transfer of glycine.[37] In the case of carboxylic acid, however, the two oxygen atoms are in principle equivalent and all hydrogen atoms near the carboxyl group in the QM region are possible candidates for the proton transfer. Thus, the sampled atomic pairs in the asymmetric coordinate in the umbrella window are interchangeable according to the possible sets. Considering all possibilities, the flexible asymmetric coordinate (FAC) is defined as follows:

$$R_{FAC} = \frac{1}{\sqrt{2}}\left(R^{\min}_{A_i-H_j} - R_{O^*-H_j}\right) \quad (2)$$

where the subscript i denotes the atomic index of all deprotonating donors, and j represents all possible candidates of the proton. The superscript min indicates the minimum distance among all $R_{A_i-H_j}$ sets. Suppose an acetic acid molecule and a water molecule are in the QM region of QM/MM model. The two oxygen atoms of acetic acid are the donors, while one carbonyl hydrogen of acetic acid and two hydrogens of QM water are the possible candidates of proton transfer. This particular definition of reaction coordinate (FAC) effectively removes problematic readsoprtion reactions and thus uniquely defines the proton transfer path of eq 1. It should be noted that FAC is a simple and effective umbrella sampling technique for the definition of the Helmholtz energy difference, and will not perturb the fundanmental solvation interactions between solutes and solvents. However, it should also be noted that there is a difference between the proton transfer mechanism, such as Grotthuss shuttling,[43] and the estimation of pK_a . The estimation of pK_a requires a free energy surface between reactants and products. The readsorption reaction of the dissociated proton to the original reactants is one of the competition reactions of proton dissociations. However, they are not necessary for calculations of the dissociation free energy surface. Therefore, selectively following the dissociation process is sufficient. FAC eliminates the chance of the readsorption reaction and uniquely connects the two reference states (reactants and products). However, this does not mean that the real proton transfer occurs through the FAC. Therefore, the FAC can be better viewed as a "technically useful coordinate" rather than as a "true proton transfer pathway". In order to obtain accurate pK_a estimation, the initial proton transfer between HA and H_2O up to the transition state, as well as the final separated state are necessary. Our FAC is a good way of describing these process.

Umbrella samplings along the flexible asymmetric coordinate (FAC) were performed with the harmonic constraint potential of the following:

$$V = \frac{k}{2}(R_{FAC} - r_0)^2 \quad (3)$$

A spherical system of QM molecules surrounded by 290 MM water molecules was prepared for the QM/MM-MD simulations. The QM molecules are HA and one quantum water, which are treated with HF/6-31G(d) level of theory for most of the molecular systems. In order to assess the quality of our quantum theory, additional QM/MM-MD simulation with MP2/cc-pVDZ level of theory was also adopted in the case of hydrogen fluoride. The TIP5P[41] was used for the 290 MM water molecules. In order to prevent evaporation of waters during long time simulations, we applied a harmonic restraint potential with a force constant of 2.0 kcal/mol/Å^2 for the boundary solvent molecules, as implemented in CHARMM.[44] Simulations on 11 windows of r_0 = −0.7, −0.5, −0.35, −0.2, 0.0, 0.35, 0.5, 0.65, 0.8, and 1.0 Å were equally performed to cover the reaction path from HB (hydrogen bonded) to CP (Coulomb pair). After that, additional 6−9 windows of r_0 =1.25−4.0 Å were performed, depending on the particular molecules to cover the reaction path from CP to DP. The force constant (k) of 100−150, 10−50, and 10−2 kcal/mol/Å^2 were used up to 1.0, 1.2−2.0, and 2.5−4.0 windows, respectively, for the umbrella sampling constraints. The one-dimensional potentials of mean force (PMF) from the umbrella samplings were obtained using the weighted histogram analysis method (WHAM).[45] Initially, NVT runs of QM/MM-MD simulations with umbrella sampling potentials over 50 ps were performed on each of the 17−20 windows at 300 K to equilibrate the systems. Then, QM/MM-MD production runs over 100 ps, also in the NVT ensemble and at 300 K, were continued from the final structures after the equilibration. A modified version of

dx.doi.org/10.1021/jp400180x | J. Phys. Chem. B 2013, 117, 6269−6275

GAMESS was used to run the QM/EFP-MD simulations. The recent distribution of GAMESS[46] contains these modifications.

The FAC as combined with umbrella sampling techniques yielded a unique PMF (potential of mean force) of the proton transfer reaction. After that, the pK_a can be directly computed from PMF using the fundamental statistical thermodynamics formalism.[47−49] For the acid dissociation reaction of eq 1, the thermodynamic equilibration constant is defined as follows:

$$K_a = \frac{(C_{a^-}/C^0)\left(C_{H_3O^+}/C^0\right)}{(C_{HA}/C^0)\left(C_{H_2O}/C^0\right)} \quad (4)$$

where, C_{A^-} is the concentration of species A^-, and C^0 is the standard concentration, which is 1 M (mole/Liter) for solute and 55.5 M for water solvent. The K_a is dimensionless and generally written without the water concentration, C_{H_2O} because the ratio of C_{H_2O}/C^0 is equal to 1. From classical statistical mechanics, given an arbitrary reaction coordinate, the probability distribution is related with the potential of mean force (PMF) as $P(r) = 4\pi r^2 e^{-\beta\omega(r)}$, where $\beta = 1/RT$ and $\omega(r)$ is the free energy (PMF) along the reaction coordinate.

The fraction of the configuration in the bound state can be computed as follows:

$$f_{HA} = \frac{\int_0^{\ddagger} P(r)\,dr}{\int_0^{\infty} P(r)\,dr} \quad (5)$$

where, ‡ denotes transition state or the dividing surface between reactant and product. The concentration of the species are expressed with this fraction and the total volume (V) as $C_{HA} = f_{HA}/V$, and $C_{A^-} = C_{H_3O^+} = (1 - f_{HA})/V$. Thus, K_a is then given by the following:

$$K_a = \frac{(1 - f_{HA})^2}{f_{HA} C^0 V} \quad (6)$$

In the limit of the infinitely dilute solution ($V \to \infty$), the fraction, $f_{HA} \to 0$ and $\int_0^{\infty} P(r)\,dr = V$. Since the simulations are calculated in particle/Å^3, the acid dissociation constant is obtained by the following:

$$K_a = 1660\left(\int_0^{\ddagger} 4\pi r^2 e^{-\beta\omega(r)}\,dr\right)^{-1} \quad (7)$$

where the unit of distance is Å and the that of free energy is RT. The number, 1660 is a factor converting particle/Å^3 to mol/L, which is calculated as follows: 1 particle $=1/6.022 \times 10^{23} = 1.66 \times 10^{-24}$ mol and $1Å^3 = 1 \times 10^{-30}m^3 = 1 \times 10^{-27}$L, so 1 particle/Å^3 $= 1.66 \times 10^{-24}$ mol/1.00×10^{-27} $L = 1660$ mol/L.

2. RESULTS AND DISCUSSIONS

2.1. Potential of Mean Force and pK_a. As described in the previous section, the potential of mean forces (PMF) along the proton transfers from HF, HCOOH, CH_3COOH, CH_3CH_2COOH, H_2CO_3, HOCl, NH_4^+, $CH_3NH_3^+$, H_2O_2, and CH_3CH_2OH to QM water were obtained by the hybrid QM/MM-MD simulations in combination with umbrella sampling techniques. The resulting PMFs of hydrogen fluoride (HF) and the other systems are presented in Figure 1 and Figure S1 of the Supporting Information, respectively. As described above, two levels of quantum theories (HF/6-31G* and MP2/cc-pVDZ) were adopted in the case of hydrogen fluoride. Overall, the two PMFs with HF/6-31G* and MP2/cc-pVDZ are nearly parallel in Figure 1. The Helmholtz energy with MP2/cc-pVDZ is slightly lower. It is generally seen that the level of the QM region does not show any significant changes in the PMF. The special structural points of HB, EB, CP, and DP along the PMF were also shown in Figure 1. HB and DP are the hydrogen bonded initial reactant and dissociated final product, respectively. EB represents the intermediate structure having equal A−H and O−H bond lengths, whereas CP is the Coulomb pair, which turned out to be the transition state. Therefore, the stability of the initially formed CP rather than the proton transfer stage (EB) is the rate-determining step. This implies that the stabilizations of the created ions require a large free energy increase.

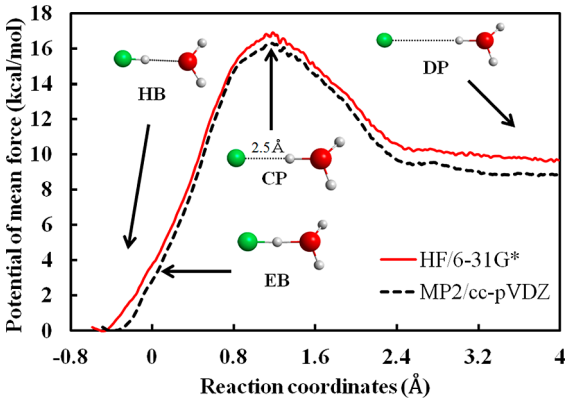

Figure 1. The potential of mean force along the proton transfer between HF and H_2O as obtained by QM/MM-MD. HB, EB, CP, and DP represent the hydrogen bond, equal bond, Coulomb pair, and dissociated pair, respectively. Both HF/6-31G* and MP2/cc-pVDZ levels of theory were used.

The pK_a values were directly calculated from PMFs by using eq 7, and the results are presented in Table 1. The values as obtained by our procedure are remarkably accurate as compared to the experiments. The maximum and root-mean-square error are 0.45 and 0.22, respectively. A comparative simulation with MP2/cc-pVDZ on a hydrogen fluoride system yielded a pK_a of 2.84, which is still within 0.5 units from experimental values. Considering the level of theory used for the solute (HF/6-31G*), the accuracy of the predicted pK_a

Table 1. Experimental and Predicted pK_a Values[a]

acid	current study	experimental
HF	3.38, **2.84**[b] (0.2)	3.18
HCOOH	3.99 (0.24)	3.75
CH_3COOH	4.81 (0.05)	4.76
CH_3CH_2COOH	4.96 (0.10)	4.86
H_2CO_3	6.31 (−0.09)	6.4
HOCl	7.84 (0.3)	7.54
NH_4^+	9.42 (0.16)	9.26
$CH_3NH_3^+$	11.11 (0.45)	10.66
H_2O_2	12.07 (0.42)	11.65
CH_3CH_2OH	15.57 (−0.32)	15.9
RMS	0.22	

[a]The numbers in parenthesis are the differences between current predictions and experiments. [b]Calculated with QM/TIP5P-MD, where MP2/cc-pVDZ level of theory was adopted for QM region. All other calculations were done with QM = HF/6-31G*.

dx.doi.org/10.1021/jp400180x | J. Phys. Chem. B 2013, 117, 6269−6275

values is remarkable. The corresponding MP2-based prediction for the pK_a of the HF molecule confirms that the predictions are relatively insensitive to the QM description of the solute. Although further extensive studies are necessary, current results exhibit a promising protocol for direct and accurate predictions of pK_a. Encouraged by our excellent agreement with experiments, the proton transfer mechanisms were further analyzed.

2.2. Solute Structures. The A−H bond lengths along the proton transfer reaction are shown in Figure 2(a). Although there is a small variation in the bond lengths depending on the solute at HB and EB, all A−H distances become nearly identical to a value of 2.5 Å at CP regardless of solute molecule. This particular distance can be a characteristic feature of proton transfer. Therefore, it is generally seen that all of the proton transfers studied here have nearly identical A−H distances in the course of proton transfer.

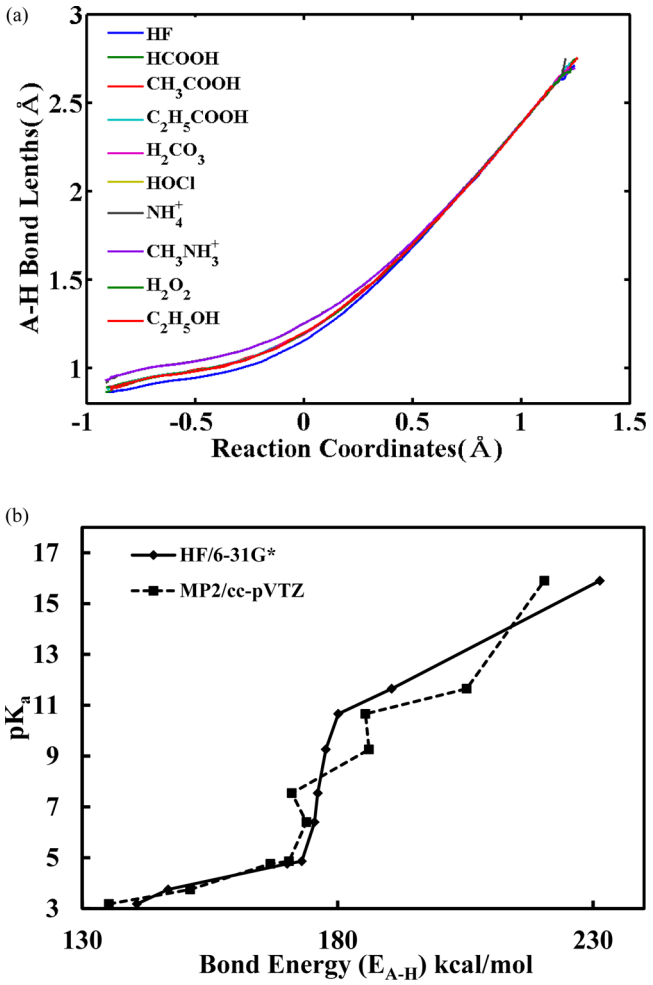

Figure 2. (a) The relation between pK_a and the A−H bond energy, which were evaluated by eq 8. Both HF/6-31G* and MP2/cc-pVTZ levels of theory were used. (b) A−H bond lengths along the PMF as collected from the corresponding windows of r_0 = −0.7−1.0.

Most of the QM-continuum computations are based on the notion that the pK_a is primarily related with the A−H bond energy. Using both HF/6-31G* and MP2/cc-pVTZ, the A−H bond energies were estimated by the following:

$$HA \rightarrow A^- + H^+ \quad (8)$$

As seen in Figure 2a, the A^----H^+ distance of 2.5 Å was applied on the product side of the above equation. The two different values agree with each other to within 5 kcal/mol. The resulting values were shown against the experimental pK_a in Figure 2(b). Although a general relation between the bond energy and pK_a exists, the correlation is not sufficiently satisfied, implying that dynamic aspects of the dissociation process should also be included for the correct pK_a. Since the gas phase deprotonation energies vary significantly with QM level of theory, their variations must be mostly canceled by the similar changes in the averaged solute−solvent interactions. However, the exact mechanism for this consistent cancellation for the set of diverse molecules used in this study will require further study. However, it should be noted that there is a fundamental difference between "free energy" and QM energy. The free energy is determined by the histogram, whereas QM energy is calculated by exact energy expression. Therefore, the "free energy" is not directly related with QM energy expression, but is instead related with various MD conditions, such as temperature and so forth.

2.3. Solvent Rearrangements. The radial distribution functions, $g(r)$, between the fluoride (F^-) and solvent water oxygen are shown in Figure 3(a). The windows corresponding to the HB, EB, CP, and DP were selectively chosen for the

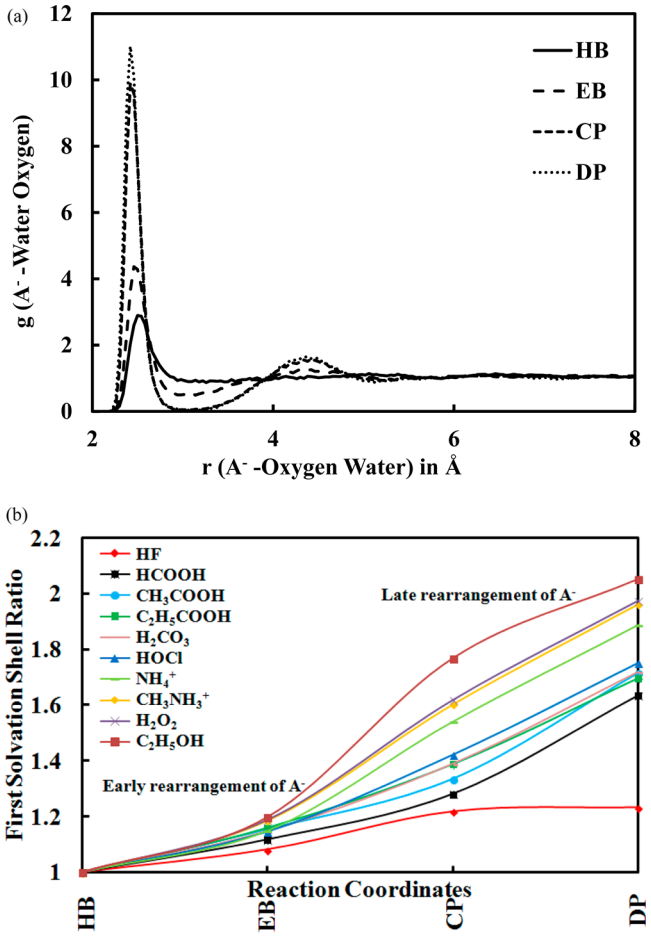

Figure 3. (a) Radial distribution functions between A and the solvent oxygen of HB, EB, CP, and DP structures. The corresponding windows are r_0 = −0.7, 0.0, 1.0, 4.0 for HB, EB, CP, and DP structures, respectively. (b) The relative first hydration shell peak area as compared to the HB.

dx.doi.org/10.1021/jp400180x | J. Phys. Chem. B 2013, 117, 6269−6275

calculations of $g(r)$. Consequently, Figure 3(a) represents the change of water structures along the PMF. The first solvation shell peak at 3.0 Å of both HB and EB becomes much larger in CP and DP, showing a large water rearrangement in the course of proton transfer. In addition, a second peak at 5.0 Å also appears in CP and DP. These observations indicate that the solvent rearrangements mostly occur between EB and CP, in which Coulombic ion pair starts to appear, suggesting that this long-range Coulomb interaction due to the ions subsequently plays a big role in the water rearrangements. In terms of bond lengths between A−H and O−H, the equal bond length EB configuration can be considered as "the solute transition state". Consequently, one can categorize the water rearrangements as before and after the EB. They can be termed as early and late rearrangements, respectively. The water rearrangements mostly occur after the EB (late rearrangement) showing that they do not directly assist the proton transfer itself but rather help in stabilizing the dissociated ions.

To quantify the degree of water rearrangements (DWR), the relative peak areas of the first peak in $g(r)$ were calculated, and the results are presented in Figure 3(b). The peak area of HB is chosen as a reference. A remarkable correlation between DWR and pK_a is seen. The ethanol, having the largest pK_a in the current study, involves the largest late rearrangement, indicating strong entropic penalties for the dissociation. However, in the case of the HF, having the smallest pK_a, the water rearrangements are rather insignificant. These observations show that the degree of water rearrangements (DWR) is highly dependent on the nature of solute. It is clear that the large pK_a of ethanol can be in part attributed to the large late rearrangement. This also strongly suggests that proper samplings of the water dynamics at dissociated regions are critical for accurate predictions of pK_a, which is lacking in the QM-continuum approaches.

3. CONCLUSIONS

We have predicted the pK_a values of HF, HCOOH, CH_3COOH, CH_3CH_2COOH, H_2CO_3, HOCl, NH_4^+, $CH_3NH_3^+$, H_2O_2, and CH_3CH_2OH in aqueous solution using QM/MM-MD in combination with an umbrella sampling technique adopting the flexible asymmetric coordinate (FAC). This unique combination yielded remarkably accurate values with the maximum and root-mean-square errors of 0.45 and 0.22 in pK_a unit, respectively, without any numerical or experimental adjustments.

In addition, our QM/MM-MD simulations provide additional insight into the details of the proton transfer mechanism and the solvation structure. According to the special structural points of HB, EB, CP, and DP along the PMF, it was found that the CP (Coulomb pair) turned out to be the transition state. Therefore, the stability of the initially formed CP rather than the proton transfer stage (EB) is the rate-determining step, implying that the stabilizations of the created ions require a large free energy increase. All A−H distances become nearly identical to a value of 2.5 Å at CP, regardless of solute molecule. This particular distance can be a characteristic feature of proton transfer.

The radial distribution functions, $g(r)$ analysis revealed that the water rearrangements mostly occur after the EB (late rearrangement) showing that they do not directly assist the proton transfer itself but rather help in stabilizing the dissociated ions. Furthermore, a remarkable correlation between DWR and pK_a is observed. The ethanol having the largest pK_a in the current study involves the largest late rearrangement, indicating strong entropic penalties for the dissociation. This showed that proper samplings of water dynamics at dissociated regions are critical for accurate predictions of pK_a.

Considering the level of theory used for the solute (HF/6-31G*), the accuracy of the predicted pK_a values is remarkable. The corresponding MP2-based prediction for the pK_a of the HF molecule, confirms that the predictions are relatively insensitive to the QM description of the solute. Since the gas phase deprotonation energies vary significantly with level of theory, they must be mostly canceled by the similar changes in the averaged solute−solvent interactions. However, the exact mechanism for this consistent cancellation for the set of diverse molecules used in this study will require further study. In any event, current results exhibit a promising protocol for direct and accurate predictions of pK_a.

■ ASSOCIATED CONTENT

Supporting Information

Predicted PMFs of HF, HCOOH, CH_3COOH, CH_3CH_2COOH, H_2CO_3, HOCl, NH_4^+, $CH_3NH_3^+$, H_2O_2, and CH_3CH_2OH. This material is available free of charge via the Internet at http://pubs.acs.org.

■ AUTHOR INFORMATION

Corresponding Author

*Tel: 053-950-5332; e-mail: thchoi@cnu.ac.kr (T.H.C.), cchoi@knu.ac.kr (C.H.C.).

Notes

The authors declare no competing financial interest.

■ ACKNOWLEDGMENTS

This work was supported by the National Research Foundation of Korea (NRF) grant to CHC funded by the Korea government (MEST) (Nos. 2007-0056341 and 2012-004812) This research was supported by Kyungpook National University Research Fund, 2012.

■ REFERENCES

(1) Zhang, S. A Reliable and Efficient First Principles-Based Method for Predicting pK_a Values. III. Adding Explicit Water Molecules: Can the Theoretical Slope Be Reproduced and pK_a Values Predicted More Accurately? *J. Comput. Chem.* **2011**, *33*, 517−526.

(2) Casasnovas, R.; Fernández, D.; Ortega-Castro, J.; Frau, J.; Donoso, J.; Muñoz, F. Avoiding Gas-Phase Calculations in Theoretical pK_a Predictions. *Theor. Chem. Acc.* **2011**, *130*, 1−13.

(3) Adam, K. R. New Density Functional and Atoms in Molecules Method of Computing Relative pK_a Values in Solution. *J. Phys. Chem. A* **2002**, *106*, 11963−11972.

(4) Zhang, S.; Baker, J.; Pulay, P. A Reliable and Efficient First Principles-Based Method for Predicting pK_a Values. 2. Organic Acids. *J. Phys. Chem. A* **2010**, *114*, 432−442.

(5) Zimmermann, M. D.; Tossell, J. A. Acidities of Arsenic (III) and Arsenic (V) Thio- and Oxyacids in Aqueous Solution using the CBS-QB3/CPCM Method. *J. Phys. Chem. A* **2009**, *113*, 5105−5111.

(6) Lu, H.; Chen, X.; Zhan, C.-G. First-Principles Calculation of pK_a for Cocaine, Nicotine, Neurotransmitters, and Anilines in Aqueous Solution. *J. Phys. Chem. B* **2007**, *111*, 10599−10605.

(7) Klicić, J. J.; Friesner, R. A.; Liu, S.-Y.; Guida, W. C. Accurate Prediction of Acidity Constants in Aqueous Solution via Density Functional Theory and Self-Consistent Reaction Field Methods. *J. Phys. Chem. A* **2002**, *106*, 1327−1335.

(8) Kallies, B.; Mitzner, R. pK_a Values of Amines in Water from Quantum Mechanical Calculations Using a Polarized Dielectric Continuum Representation of the Solvent. *J. Phys. Chem. B* **1997**, *101*, 2959−2967.
(9) Chipman, D. M. Computation of pK_a from Dielectric Continuum Theory. *J. Phys. Chem. A* **2002**, *106*, 7413−7422.
(10) Liptak, M. D.; Gross, K. C.; Seybold, P. G.; Feldgus, S.; Shields, G. C. Absolute pK_a Determinations for Substituted Phenols. *J. Am. Chem. Soc.* **2002**, *124*, 6421−6427.
(11) Liptak, M. D.; Shields, G. C. Accurate pK_a Calculations for Carboxylic Acids Using Complete Basis Set and Gaussian-n Models Combined with CPCM Continuum Solvation Methods. *J. Am. Chem. Soc.* **2001**, *123*, 7314−7319.
(12) Schmidt am Busch, M.; Knapp, E.-W. Accurate pK_a Determination for a Heterogeneous Group of Organic Molecules. *ChemPhysChem* **2004**, *5*, 1513−1522.
(13) Barone, V.; Improta, R.; Rega, N. Computation of Protein pK_a Values by an Integrated Density Functional Theory/Polarizable Continuum Model Approach. *Theor. Chem. Acc.* **2004**, *111*, 237−245.
(14) Pliego, J. R.; Riveros, J. M. Theoretical Calculation of pK_a Using the Cluster−Continuum Model. *J. Phys. Chem. A* **2002**, *106*, 7434−7439.
(15) Liptak, M. D.; Shields, G. C. Experimentation with Different Thermodynamic Cycles Used for pK_a Calculations on Carboxylic Acids Using Complete Basis Set and Gaussian-n Models Combined with CPCM Continuum Solvation Methods. *Int. J. Quantum Chem.* **2001**, *85*, 727−741.
(16) Fu, Y.; Liu, L.; Li, R.-Q.; Liu, R.; Guo, Q.-X. First-Principle Predictions of Absolute pK_a's of Organic Acids in Dimethyl Sulfoxide Solution. *J. Am. Chem. Soc.* **2004**, *126*, 814−822.
(17) Ding, F.; Smith, J. M.; Wang, H. First-Principles Calculation of pK_a Values for Organic Acids in Nonaqueous Solution. *J. Org. Chem.* **2009**, *74*, 2679−2691.
(18) Pliego, J. R.; Riveros, J. M. The Cluster−Continuum Model for the Calculation of the Solvation Free Energy of Ionic Species. *J. Phys. Chem. A* **2001**, *105*, 7241−7247.
(19) Pliego, J. R., Jr; Riveros, J. M. Gibbs Energy of Solvation of Organic Ions in Aqueous and Dimethyl Sulfoxide Solutions. *Phys. Chem. Chem. Phys.* **2002**, *4*, 1622−1627.
(20) Kelly, C. P.; Cramer, C. J.; Truhlar, D. G. Aqueous Solvation Free Energies of Ions and Ion−Water Clusters Based on an Accurate Value for the Absolute Aqueous Solvation Free Energy of the Proton. *J. Phys. Chem. B* **2006**, *110*, 16066−16081.
(21) Bryantsev, V. S.; Diallo, M. S.; Goddard, W. A., III Calculation of Solvation Free Energies of Charged Solutes Using Mixed Cluster/Continuum Models. *J. Phys. Chem. B* **2008**, *112*, 9709−9719.
(22) Jia, Z.-K.; Du, D.-M.; Zhou, Z.-Y.; Zhang, A.-G.; Hou, R.-Y. Accurate pK_a Determinations for Some Organic Acids Using an Extended Cluster Method. *Chem. Phys. Lett.* **2007**, *439*, 374−380.
(23) Wang, X.-X.; Fu, H.; Du, D.-M.; Zhou, Z.-Y.; Zhang, A.-G.; Su, C.-F.; Ma, K.-S. The Comparison of pK_a Determination between Carbonic Acid and Formic Acid and Its Application to Prediction of the Hydration Numbers. *Chem. Phys. Lett.* **2008**, *460*, 339−342.
(24) Casasnovas, R.; Frau, J.; Ortega-Castro, J.; Salvà, A.; Donoso, J.; Muñoz, F. Absolute and Relative pK_a Calculations of Mono and Diprotic Pyridines by Quantum Methods. *J. Mol. Struct.-Theochem.* **2009**, *912*, 5−12.
(25) Ho, J.; Coote, M. L. A Universal Approach for Continuum Solvent pK_a Calculations: Are We There Yet? *Theor. Chim. Acta* **2010**, *125*, 3−21.
(26) Kelly, C. P.; Cramer, C. J.; Truhlar, D. G. Adding Explicit Solvent Molecules to Continuum Solvent Calculations for the Calculation of Aqueous Acid Dissociation Constants. *J. Phys. Chem. A* **2006**, *110*, 2493−2499.
(27) Eckert, F.; Diedenhofen, M.; Klamt, A. Towards a First Principles Prediction of pK_a: COSMO-RS and the Cluster-Continuum Approach. *Mol. Phys.* **2010**, *108*, 229−241.
(28) Abramson, R.; Baldridge, K. K. Defined-Sector Explicit Solvent in the Continuum Model Approach for Computational Prediction of pK_a. *Mol. Phys.* **2012**, *110*, 2401−2412.
(29) Davies, J. E.; Doltsinis, N. L.; Kirby, A. J.; Roussev, C. D.; Sprik, M. Estimating pK_a Values for Pentaoxyphosphoranes. *J. Am. Chem. Soc.* **2002**, *124*, 6594−6599.
(30) Ivanov, I.; Chen, B.; Raugei, S.; Klein, M. L. Relative pK_aValues from First-Principles Molecular Dynamics: The Case of Histidine Deprotonation. *J. Phys. Chem. B* **2006**, *110*, 6365−6371.
(31) Cheng, J.; Sulpizi, M.; Sprik, M. Redox Potentials and pK_a for Benzoquinone from Density Functional Theory Based Molecular Dynamics. *J. Chem. Phys.* **2009**, *131*, 154504.
(32) Mangold, M.; Rolland, L.; Costanzo, F.; Sprik, M.; Sulpizi, M.; Blumberger, J. Absolute pK_a Values and Solvation Structure of Amino Acids from Density Functional Based Molecular Dynamics Simulation. *J. Chem. Theory Comput.* **2011**, *7*, 1951−1961.
(33) Masunov, A.; Lazaridis, T. Potentials of Mean Force between Ionizable Amino Acid Side Chains in Water. *J. Am. Chem. Soc.* **2003**, *125*, 1722−1730.
(34) Car, R.; Parrinello, M. Unified Approach for Molecular Dynamics and Density-Functional Theory. *Phys. Rev. Lett.* **1985**, *55*, 2471−2474.
(35) Komeiji, Y.; Nakano, T.; Fukuzawa, K.; Ueno, Y.; Inadomi, Y.; Nemoto, T.; Uebayasi, M.; Fedorov, D. G.; Kitaura, K. Fragment Molecular Orbital Method: Application to Molecular Dynamics Simulation, "Ab Initio FMO-MD". *Chem. Phys. Lett.* **2003**, *372*, 342−347.
(36) Field, M. J.; Bash, P. A.; Karplus, M. A Combined Quantum Mechanical and Molecular Mechanical Potential for Molecular Dynamics Simulations. *J. Comput. Chem.* **1990**, *11*, 700−733.
(37) Choi, C. H.; Re, S.; Feig, M.; Sugita, Y. Quantum Mechanical/Effective Fragment Potential Molecular Dynamics (QM/EFP-MD) Study on Intra-Molecular Proton Transfer of Glycine in Water. *Chem. Phys. Lett.* **2012**, *539*−*540*, 218−221.
(38) Ghosh, M. K.; Re, S.; Feig, M.; Sugita, Y.; Choi, C. H. Interionic Hydration Structures of NaCl in Aqueous Solution: A Combined Study of Quantum Mechanical Cluster Calculations and QM/EFP-MD Simulations. *J. Phys. Chem. B* **2013**, *117*, 289−295.
(39) Ghosh, M. K.; Uddin, N.; Choi, C. H. Hydrophobic and Hydrophilic Associations of a Methanol Pair in Aqueous Solution. *J. Phys. Chem. B* **2012**, *116*, 14254−14260.
(40) Ghosh, M. K.; Lee, J.; Choi, C. H.; Cho, M. Direct Simulations of Anharmonic Infrared Spectra Using Quantum Mechanical/Effective Fragment Potential Molecular Dynamics (QM/EFP-MD): Methanol in Water. *J. Phys. Chem. A* **2012**, *116*, 8965−8971.
(41) Mahoney, M.; Jorgensen, W. A Five-Site Model for Liquid Water and the Reproduction of the Density Anomaly by Rigid, Nonpolarizable Potential Functions. *J. Chem. Phys.* **2000**, *112*, 8910−8922.
(42) Bolhuis, P. G.; Chandler, D.; Dellago, C.; Geissler, P. L. Transition Path Sampling: Throwing Ropes over Rough Mountain Passes, in the Dark. *Annu. Rev. Phys. Chem.* **2002**, *53*, 291−318.
(43) Markovitch, O.; Chen, H.; Izvekov, S.; Paesani, F.; Voth, G. A.; Agmon, N. Special Pair Dance and Partner Selection: Elementary Steps in Proton Transport in Liquid Water. *Chem. Rev.* **2008**, *112*, 9456−9466.
(44) Brooks, B. R.; Bruccoleri, R. E.; Olafson, B. D.; States, D. J.; Swaminathan, S.; Karplus, M. CHARMM: A Program for Macromolecular Energy, Minimization, And Dynamics Calculations. *J. Comput. Chem.* **1983**, *4*, 187−217.
(45) Grossfield, A. "WHAM: The Weighted Histogram Analysis Method." http://membrane.urmc.rochester.edu/content/wham 2012.
(46) Schmidt, M. W.; Baldridge, K. K.; Boatz, J. A.; Elbert, S. T.; Gordon, M. S.; Jensen, J. H.; Koseki, S.; Matsunaga, N.; Nguyen, K. A.; Su, S.; Windus, T. L.; Dupuis, M.; Montgomery, J. A. General Atomic and Molecular Electronic Structure System. *J. Comput. Chem.* **1993**, *14*, 1347−1363.
(47) Chandler, D. G. *Introduction To Modern Statistical Mechanics*; Oxford University Press: New York, 1987.

(48) Maupin, C. M.; Wong, K. F.; Soudackov, A. V.; Kim, S.; Voth, G. A. A Multistate Empirical Valence Bond Description of Protonatable Amino Acids. *J. Phys. Chem. A* **2006**, *110*, 631−639.
(49) Chen, J.; Brooks, C. L.; Scheraga, H. A. Revisiting the Carboxylic Acid Dimers in Aqueous Solution: Interplay of Hydrogen Bonding, Hydrophobic Interactions, and Entropy. *J Phys Chem B* **2008**, *112*, 242−249.